Flame Retardant Polyester by Combination of organophosphorus Compounds and a NOR Radical Forming Agent

Daniela Goedderz[1,2], Lais Weber[1,2], Daniel Markert[1], Alexander Schießer[3], Claudia Fasel[4], Ralf Riedel[4], Volker Altstädt[5], Christian Bethke[5], Olaf Fuhr[6], Manfred Döring[2]*

[1] Ernst-Berl Institute for Chemical Engineering and Macromolecular Science, Technische Universität Darmstadt, Alarich-Weiss-Straße 4, Darmstadt, D-64287, Germany

[2] Fraunhofer Institute for Structural Durability and System Reliability LBF, Schlossgartenstraße 6, Darmstadt, D-64289, Germany

[3] Mass Spectrometry, Department of Chemistry, Technische Universität Darmstadt, Alarich-Weiss-Straße 4, Darmstadt, D-64287, Germany

[4] Institut für Materialwissenschaft, Technische Universität Darmstadt, Otto-Bernd-Straße 3, Darmstadt, D-64287, Germany

[5] Department of Polymer Engineering, University of Bayreuth, Universitätsstraße 30, Bayreuth, D-95447, Germany

[6] Institut für Nanotechnologie (INT) und Karlsruher Nano-Micro-Facility (KNMF), Karlsruher Institut für Technologie (KIT), Hermann-von-Helmholtz-Platz 1,76344 Eggenstein-Leopoldshafen, Germany

Correspondence to: Manfred Döring (E-mail: *Manfred.doering@lbf.fraunhofer.de*)

ABSTRACT

Polymer materials with different surface-to-volume ratios require different mechanisms of flame retardants regarding condensed phase and gas phase activity. The flame retardant formulations in poly(ethylene terephthalate) (PET) are investigated regarding to a condensed phase and gas phase activity by using TGA, TG-MS, TG-FTIR, UL94 and SEM-EDX measurements. The flame retardant formulations containing phosphates, phosphonates and phosphinates as flame retardants are analyzed by using a simultaneous analysis consisting of a DTA-TGA device which is insitu coupled to FTIR and MS. All analysis methods show a gas phase activity for the phosphonate (PCO 910), a condensed phase activity for the phosphate (SPDPP) and a mixed condensed and gas phase activity for the new synthesized phosphate and DOPO containing flame retardant SPDPDOM. The fire behavior of PCO 910 can be improved by adding a NOR radical forming agent (NOR-RF) reaching a total amount of 3wt% of both active agents for a UL94 V-0 classification in PET.

INTRODUCTION

Poly(ethylene terephthalate) (PET) offers a broad portfolio of applications for thin-walled or bulk materials and is a combustible material which requires tailor-made flame retardant solutions. Thin-walled applications like foils, fibers and foams are very sensitive to changes of the melt viscosity by

additives like flame retardants restricting their use. For this purpose it is preferable to choose low loadings of flame retardants resulting in lower impairments of the melt viscosity, foamability or mechanical properties of the finished product. In this work the total amount of flame retardants was kept as low as possible. High processing temperatures of PET (max 300 °C) call for flame retardant agents which have an adequate thermostability.[1] Some phosphorus containing flame retardants like Aflammit® PCO 910 or Exolit® OP 950 satisfy these requirements. There are very few radical forming agents which meet this requirement. NOR radical forming agents include Flamestab NOR 116 and ester of N-hydroxyimides.[2] The selected NOR radical forming agent thereof has a suitable thermostability for an extrusion process with PET. The development of non-halogenated as well as non-volatile flame retardants is getting more and more important due to bans of certain toxic flame retardants.[3]

Phosphorus based flame retardants can be gas phase active and/or condensed phase active depending on the chemical environment of the phosphorus atom and the structural characteristics of the matrix polymer. The increasing oxygen environment of the phosphorus atom in flame retardants results in an increasing charring effect. On the other hand an increasing carbon or hydrogen environment of the phosphorus atom in flame retardants result in a predominantly gas phase activity as mentioned in many studies before.[4] During the combustion process of organic polymeric materials highly reactive H- and OH-radicals are generated as flame propagating species. Phosphorus based flame retardants which decompose with evolution of phosphorus based radicals decrease the concentration of H- and OH-radicals thus being not able to maintain the combustion process (flame poisoning).[4b, 5]

We examined the flame retardant efficiency and the thermal properties of different phosphorus based flame retardants such as phosphonates, phosphates and phosphinates individually and in combination with a NOR radical forming agent (NOR-RF, Figure 1). The phosphate based flame retardants are all derivatives of a spirocyclic pentaerythritol compound. The spirobis(pentaerythritol chlorophosphate) (SPDPC) can be used easily for esterification. Pentaerythritol spirobis(methylphosphonate) (PCO 910) is commercial available and used among other things as flame retardant for polyesters. By the esterification of 6-oxide-6-H-dibenz[c,e][1,2]oxaphopshorin-6-methanol) (DOPO-MeOH) with SPDPC we synthesized a new flame retardant unifiying a phosphate and a DOPO moiety and thus gas phase and condensed phase activity in one molecule. DOPO-based polymers realized in Heim® by Toboyo are intrinsically flame retardant fibers.[6] PO radicals were detected for flame retardants indicating a gas phase activity using a TGA/DTA device which is insitu coupled to FTIR and MS. In this work a combination of a flame retardant with gas phase activity was combined with NOR radical forming agent characterized by its high thermostability enhancing the flame retardancy with only a total loading of 3% of active agents.
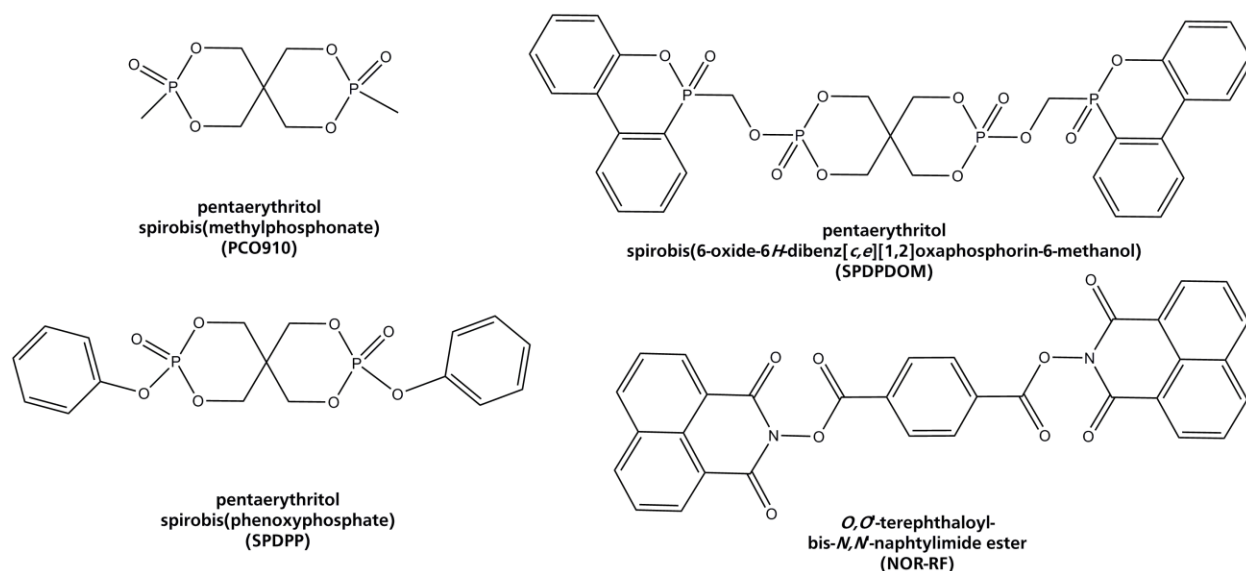
FIGURE 1 Molecular structures of the phosphonate based (PCO910), phosphate based (SPDPP), DOPO-/phosphate based (SPDPDOM) flame retardants as well as the NOR radical forming agent (NOR-RF).

EXPERIMENTAL

Material

PET (BISNEINEX®) was provided by Equipolymers in Italy. Aflammit® PCO 910 was provided by Thor in Germany. Unless stated otherwise, solvents and chemicals were obtained from ACROS Organics™ and used without further purification. 6*H*-Dibenz[*c,e*][1,2]oxaphosphorin-6-methanol-6-oxide (DOPO-MeOH) was supplied by Metadynea Austria GmbH.

General procedure

All experiments were carried out under nitrogen atmosphere and dry solvents were used. NMR data were obtained on a Bruker NanoBay 300 spectrometer. Chemical shifts are reported as δ values relative to the solvent peak in ppm. Trimethylsilane was used as a standard.

Single crystals of $C_{17}H_{18}O_8P_2$ [SPDPP] were obtained through precipitation from water/methanol. Diffraction data of a suitable crystal were collected on a STOE STADIVARI diffractometer. The crystal was kept at 150.15 K during data collection. Using Olex2[7], the structure was solved with the ShelXS[8] structure solution program using Direct Methods and refined with the ShelXL[9] refinement package using Least Squares minimization. Structural data are in agreement with those published by Heinemann et al.[10] in 1994.

The phosphorus content was determined using a scanning electron microscope (Jeol JSM 6400, 20 kV acceleration voltage and 40x magnification) equipped with an energy-dispersive X-ray spectrometer (EDX, EDAX Apollo).

Thermodesorption-MS experiments were made using a Finnigan MAT 95 with a constant heating rate of 25 K/min in a temperature range of 40-400 °C.

Thermogravimetric analysis was carried out using a TGA Q500 from TA Instruments with a heating rate of 10 K/min under constant nitrogen or air atmosphere.

The simultaneous thermal analysis was carried out using a TGA/DTA (STA 449C Jupiter®, Netzsch Gerätebau GmbH, Selb) coupled to FTIR (Bruker Tensor 27) and MS (QMS 403C Aëolos®) at a constant heating rate of 10 K/min in a temperature range of 35-600 °C.

Compounding was carried out using a corotating twin-screw extruder (Thermo Scientific Process 11 from Fisher Scientific, screw diameter: 11 mm) with a screw rotation speed of 150 rpm. The first temperature zone was set as 240 °C, all other temperature zones were set as 270 °C. The melt strand was cooled with a water bath and pelletized in a pelletizing system (Varicut Granulator).

The UL94 samples were obtained by hot pressing (Collin) of the compounds at 270 °C and 5 bar for 5 minutes. The UL 94 vertical burning test setup was done using a Wazau burning chamber according to DIN IEC 60,695-11-10 with a 50 W burner flame.

Synthesis of 3,9-dichloro-2,4,8,10-tetraoxa-3,9-diphosphaspiro-5,5-undecane-3,9-dioxid (SPDPC)[11]

A flame dried three-neck round-bottom glass flask was equipped with a reflux condenser and a magnetic stirrer. 60 g (441 mmol, 1.0 Aq.) of pentaerythritol and 189.11 g (1233 mmol, 2.8 Aq.) of phosphoroxychloride were added and heated to 75 °C for 4 h. The reaction mixture was heated to 105 °C for 6 h and cooled to RT. The colorless residue was filtered off and washed with chloroform. The obtained solid was dried in vacuo for 24 h. Yield: 81%

^{1}H NMR (300.38 MHz, 298 K, CDCl$_3$): δ = 4.59 (ddd, 1H; J = 28.5 Hz, 12.4 Hz, 2.8 Hz); 4.44-4.27 (m, 1H); 4.19-3.88 (m, 2H) ppm. ^{31}P NMR (121.60 MHz/ 298 K/ CDCl$_3$): δ = -3.09 ppm.

Synthesis of 3,9-bis(phenoxy)-2,4,8,10-tetraoxa-3,9-diphosphaspiro-5,5-undecane-3,9-dioxide (SPDPP)[11]

A flame dried 250 mL three-neck round-bottom glass flask was equipped with a reflux condenser and a magnetic stirrer. 40 g (134.7 mmol, 1.0 Aq.) SPDPC, 28 g (297.5 mmol, 2.2 Aq.) phenol and 380 mL acetonitrile were added. Under vigorous stirring 42 mL (298.8 mmol, 2.2 Aq.) triethylamine was added drop by drop. After 6 h the precipitated white solid was collected by filtration and washed with water and dried in vacuo at 60 °C. Yield: 53%

^{1}H NMR (300.38 MHz, 298 K, DMSO-d6): δ = 7.50-7.26 (m, 10 H); 4.85-4.41 (m, 8H) ppm. ^{31}P NMR (121.60 MHz/ 298 K/ DMSO-d6): δ = -13.60 ppm. TGA: T$_{98}$ = 405 °C, T$_o$ = 530 °C.

Crystal Data for C$_{17}$H$_{18}$O$_8$P$_2$ (M =412.25 g/mol): orthorhombic, space group Pna2$_1$ (no. 33), a = 11.4710(3) Å, b = 6.1955(2) Å, c = 25.7028(7) Å, V = 1826.66(9) Å^3, Z = 4, T = 150.15 K, μ(GaKα) = 1.663 mm^{-1}, Dcalc = 1.499 g/cm^3, 11487 reflections measured (5.984° ≤ 2Θ ≤ 114.982°), 3743 unique (R$_{int}$ = 0.0328, R$_{sigma}$ = 0.0237) which were used in all calculations. The final R$_1$ was 0.0498 (I > 2σ(I)) and wR$_2$ was 0.1407 (all data).

Synthesis of 3,9-bis(phenoxy)-2,4,8,10-tetraoxa-3,9-diphosphaspiro-5,5-undecane-3,9-dioxide (SPDPDOM)

A flame dried 500 mL three-neck round-bottom glass flask was equipped with a reflux condenser and a magnetic stirrer. 12.16 g (40.94 mmol, 1 Aq.) SPDPC, 21.17 g (85.99 mmol, 2.1 Aq.) DOPO-MeOH and 200 mL acetonitrile were added. Under vigorous stirring 12 mL (86.10 mmol, 2.1 Aq.) triethylamine was added drop by drop. After 12 h at 80 °C the precipitated white solid was collected by filtration and washed with water and dried in vacuo. Yield: 89%

^{1}H NMR (300.38 MHz, 298 K, DMSO-d6): δ = 8.34-8.25 (dd, J = 21.96; 7.75 Hz, 4 H); 8.09-8.06 (m, 2H); 7.93-7.87 (td, J = 8.22; 7.52; 1.41 Hz, 2H); 7.72-7.67 (t, J = 7.50; 7.50 Hz, 2H); 7.52-7.47 (m, 2H); 7.39-7.35 (m, 4H); 4.94-4.72 (m, 4H); 4.26-4.16 (m, 2H); 3.86-3.82 (d, J = 12.12 Hz, 2H); 3.64-3.59 (dd, J = 11.72;

2.22 Hz, 2H); 3.30-3.26 (d, J = 11.89 Hz, 2H[31]P NMR (121,60 MHz/ 298 K/ DMSO-d6): δ = -8.47 ppm (d; J = 31.75 Hz); 27.29 ppm (d; J = 31.75 Hz). TGA: T_1 = 293 °C, T_{95} = 357 °C.

Synthesis of *N*-Hydroxynaphthalimide[12]

A flame dried 1000 mL three-neck round-bottom glass flask is equipped with a magnetic stirrer. 42.08 g (605.51 mmol, 1.5 Aq.) Hydroxylamine hydrochloride was dissolved in 600 mL pyridine. 80.00 g (403.67 mmol, 1.0 Aq.) 1,8-naphthalic acid anhydride were added and the reaction mixture is stirred for 20 h at RT. The precipitate is filtered of and washed with water. Yield: 79%
^{1}H NMR (300.38 MHz, 298 K, DMSO-d6): δ = 10.76 (s, 1 H), 8.52-8.45 (dd, 4H), 7.91-7.86 (m, 2H).

Synthesis of O,O'-Terephthaloyl-bis-N,N'-naphthalimide ester (NOR-RF)[12]

A flame dried 2000 mL three-neck round-bottom glass flask is equipped with a reflux condenser and a magnetic stirrer. 50.00 g (234.54 mmol, 2.5 Aq.) *N*-Hydroxynaphthalimide were dissolved in 1500 mL pyridine at 45 °C. 19.05 g (93.82 mmol, 1.0 Aq.) terephthalic acid dichloride was added and the reaction mixture is stirred at 45 °C for 1 h and then stirred at RT for 20 h. The precipitate is filtered off and washed with water. Yield: 75%
MS m/z: 556.24 u.TGA: T_1 = 237 °C, T_{95} = 349 °C.

RESULTS AND DISCUSSION

SPDPC was synthesized according to the literature[11] from pentaerythritol and phosphorus oxychloride. Aflammit® PCO 910 is a commercial available phosphonate from Thor. The flame retardants SPDPP and SPDPDOM are synthesized from SPDPC and phenol respectively DOPO-MeOH.

Crystal structure of SPDPP

Single crystals were obtained from SPDPP and the crystal structure was investigated (Figure 2). SPDPP crystallizes in an orthorhombic crystal system with the space group *Pna2₁*. The planes of the phenol rings are forming an angle of 8.16° and the six-membered rings of the spirobisphosphate ring are twisted against one another about 89.12°. The six-membered aliphatic rings of the spirobisphosphonate adopt a flattened chair confirmation with the P=O group in the equatorial position. The crystal structures of 3,9-dichloro-2,4,8,10-tetraoxa-3,9-diphosphaspiro[5.5]undecane-3,9-dione and 3,9-diphenoxy-2,4,8,10-tetraoxa-3,9-diphosphaspiro[5.5]undecane-3,9-dioxide have been reported by Zhan et al.[13] and Heinemann et al.[10] in 2010 and 1994. Cyclic phosphate esters like 2-Oxo-2-phenoxy-1,3,2-dioxaphosphorinane reported by Geise et al. show very similar O-P-O-bonding angles as the corresponding spirobisphosphate SPDPP.[14] For SPDPDOM no crystals were obtained but the crystal structure is expected to be comparable to SPDPP.
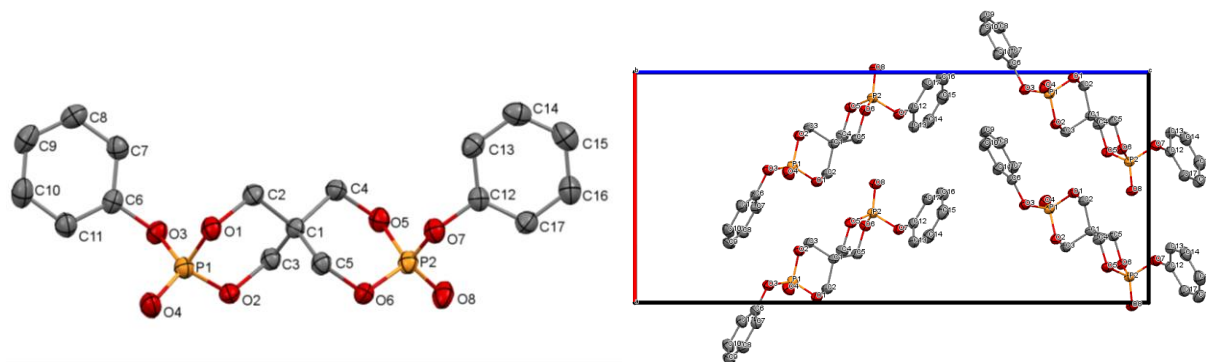
FIGURE 2 Molecular structure of SPDPP. Crystal packing of SPDPP viewed along the b axis. Hydrogen atoms were omitted for clarity.

Flame retardant formulations in PET

Table 1 summarizes the composition of the flame retardant formulations. The phosphorous atoms of the flame retardants PCO 910, SPDPP and SPDPDOM have different chemical environments. SPDPDOM includes phosphate as well as DOPO moieties and an overall phosphorus content of 17.32%. PCO 910 has a phosphorous content of 24.18% whereas SPDPP contains 15.02% phosphor.

TABLE 1 Investigated compositions of flame retarded poly(ethylene terephthalate) formulations containing different phosphorus compounds and the NOR radical forming agent.

	Amount of Flame Retardants and NOR Radical forming agent				Calculated phosphorus content [%]
#	PCO 910 [%]	SPDPP [%]	SPDPDOM [%]	NOR-RF [%]	
1	-	-	-	-	-
2	5	-	-	-	1.29
3	10	-	-	-	2.42
4	-	10	-	-	1.50
5	-	-	-	5	-
6	2	-	-	1	0.48
7	-	2	-	1	0.30
8	-	-	2	-	0.35
9	-	-	10	-	1.73
10	2	-	-	-	0.48
11	-	2	-	-	0.30

Insitu thermal analysis of flame retardant formulations

Figure 3 shows TGA curves for the single flame retardant components under nitrogen (left diagram) and under air atmosphere (right diagram). The TGA results indicate a condensed phase activity for SPDPP and a gas phase activity for PCO 910 due to the amount of residues at 600 °C. The phosphonate has a residue of 6% at 600 °C whereas the corresponding phenoxy phosphate has a residue of 37% at 600 °C. Both phosphorous compounds degrade in a single step. The thermal behaviour of PCO 910 under air atmosphere is similar to that under nitrogen atmosphere with slightly more residue at 600 °C. Neat SPDPP decomposes more rapidly and with less residue at 600 °C under air atmosphere due to oxidation processes which is in accordance to the literature.[11b, 15] The decomposition of SPDPDOM starts at lower temperatures under air atmosphere than under inert atmosphere showing a further degradation step starting at 600 °C. The TGA curve under air atmosphere of NOR-RF shows a further oxidation of the char residue especially at 600 °C. No significant differences of the TGA curves of the neat flame retardants can be observed, so further investigations of the thermal behaviour were carried out under nitrogen atmosphere.
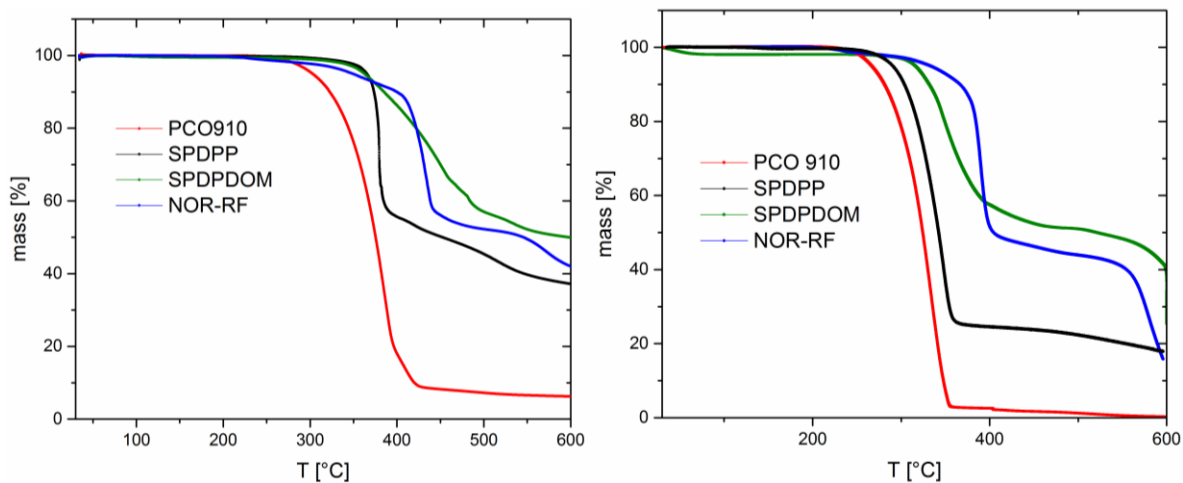

FIGURE 3 Thermogravimetric analysis of neat flame retardants PCO 910, SPDPP, SPDPDOM and the NOR radical forming agent (NOR-RF) at 10 K/min under nitrogen (left diagram). Thermogravimetric analysis of neat flame retardants PCO 910, SPDPP, SPDPDOM and the NOR radical forming agent (NOR-RF) at 10 K/min under air atmosphere (right diagram).

Table 2 summarizes the thermal properties of the investigated flame retardants and flame retardant formulations. It can be clearly observed that the incorporation of 10wt% of SPDPP in PET leads to a char formation of + 10-13% at 600 °C in comparison to neat PET and the incorporation of the same amount of phosphonate flame retardant. An increasing amount of the remaining residues at 600 °C of the flame retardant formulations is an indication for a condensed phase activity. The temperature of the maximum decomposition rate ($T_{max\ dec\ rate}$) is most influenced and decreased by the incorporation of the phosphate into PET. The phosphonate flame retardants in PET lead to an increased temperature of the decomposition maximum (435-444 °C) in comparison to neat PET. 5% PCO 910 and 10% SPDPP having comparable phosphorus contents of about 1.3-1.5% show a difference in the remaining residues at 600 °C of about 9%.

TABLE 2 Thermal properties of the flame retardant formulations in PET by simultaneous thermal analysis (TGA-DTA).

#	composition	$T_{1\%}$ [°C]	T_m [°C]	$T_{max\ dec\ rate}$ [°C]	Residue at 600 °C [%]
0-1	PCO 910	267.05	250.03	386.29	6
0-2	SPDPP	315.54	197.31	379.65	37
0-3	SPDPDOM	293.33	-	457.13	50
0-4	NOR-RF	237.33	-	423.72	42
1	PET	375.58	243.99	429.48	16
2	2% PCO 910	368.35	244.20	443.50	17
3	5% PCO 910	288.29	242.14	444.15	19
4	10% PCO 910	155.39	239.6	435.29	19
5	2% SPDPP	375.79	244.60	436.46	24
6	10% SPDPP	367.94	241.31	394.24	30
7	2% SPDPDOM	378.76	247.12	440.64	24
8	5% RF	316.59	246.75	440.42	16
9	2% PCO 910 + 1% NOR-RF	327.38	244.56	442.89	17
10	2% SPDPP + 1% NOR-RF	353.29	244.51	436.63	23
11	8% PCO 910 + 4% NOR-RF	300.10	240.29	441.92	20

The neat NOR-RF compound as NOR radical forming agent generates a residue of 42% at 600 °C (Table 2) due to the high aromatic content of the NOR-RF that will remain in the condensed phase in case of fire. Figure 4 shows the TGA curves for all flame retardant formulations in PET (upper left diagram). The turning points of the phosphate containing formulations 10% SPDPP and 10% SPDPDOM have lower corresponding temperatures than comparable phosphonate formulations. As expected, the quantities of the remaining residues of the phosphate containing formulations are higher than those of phosphonate containing flame retardant formulations with comparable phosphorus contents. As can be seen in the upper right diagram a mass loss step of about 5% for the formulation containing 5% NOR-RF takes place.
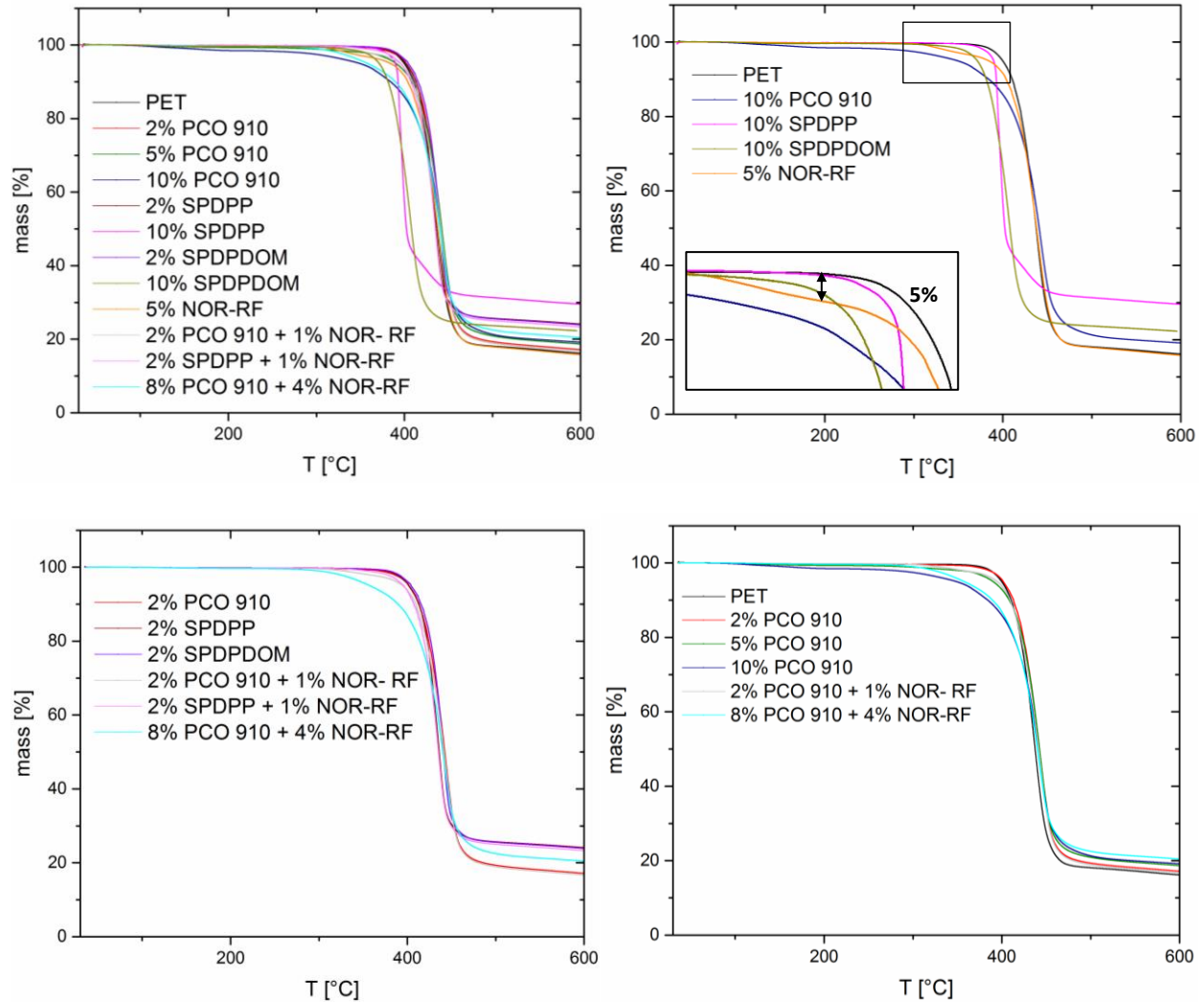
FIGURE 4 TGA curves of the flame retardant formulations (PET, 2% PCO 910, 5% PCO 910, 10% PCO 910, 2% SPDPP, 10% SPDPP, 2% SPDPDOM, 10% SPDPDOM, 5% NOR-RF, 2% PCO 910 + 1% NOR-RF, 2% SPDPP + 1% NOR-RF, 8% PCO 910 + 4% NOR-RF) under nitrogen and a heating rate of 10 K/min (top left diagram). For reasons of clarity top right, bottom left and right diagrams show selected curves of the flame retardant formulations.

The NOR-RF degrades first which also can be observed by the release of carbon dioxide in TG-FTIR experiments (Figure 5). There are two clear and separate CO_2-release steps. The combination of 8% PCO 910 and 4% NOR-RF shows also a degradation in two steps, but they are more close and the degradation of the NOR-RF starts 15 °C higher than without PCO 910 and has no clear maximum.
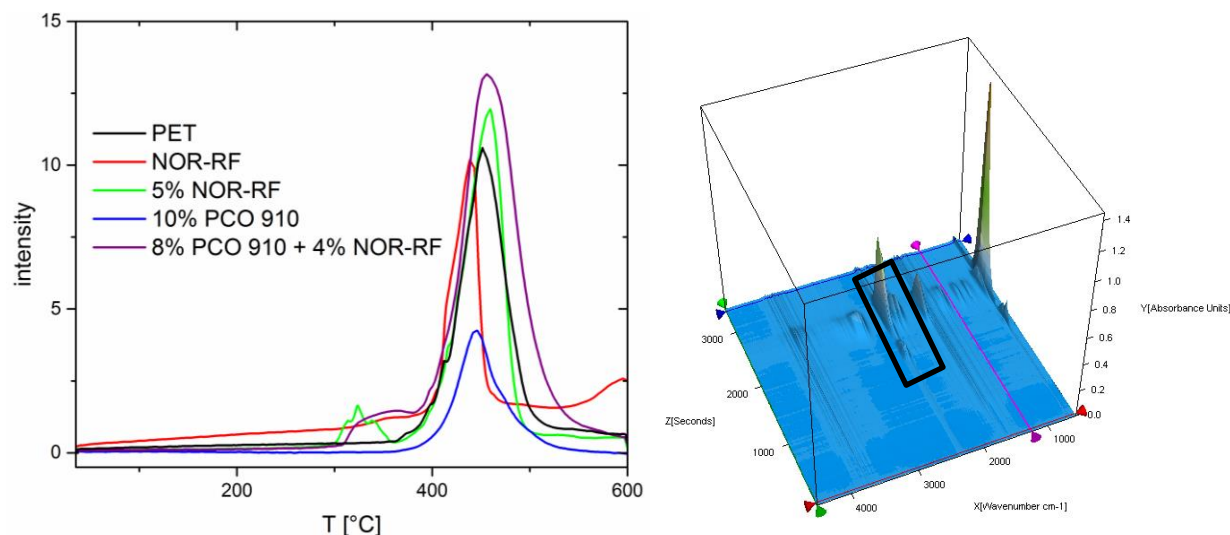
FIGURE 5 TG-FTIR curve (left diagram) showing the CO_2 release intensity of PET flame retardant formulations containing neat PET, neat NOR-RF, 5% NOR-RF, 10% PCO 910 and 8% PCO 910 + 4% NOR-RF in PET (integral traces at 2378-2302 cm^{-1} (CO_2)). 3D-FTIR spectroscopy of PET containing 5% NOR-RF (right diagram).

The fragmentation of the spirobis(phosphate) and spirobis(phosphonate) flame retardant in TG-MS analysis is different. The fragmentation of spirocyclic phosphonates in MS experiments is already investigated and described in the literaure.[16] Some found fragments of the decomposition of PCO 910 are in accordance to the decomposition pathway described in the literature. The decomposition of the phosphonate PCO 910 shows the release of methanal whereas the phosphate derivative releases phenol and its derivatives during the decomposition process. These two decomposition species can be obtained also by TG-FTIR analysis. The formulation containing the phosphate in PET leads to no detection of phenol and its derivatives in TG-MS experiments which indicate that no release of phenol takes place. As found by simultaneous TG-FTIR and TG-MS experiments, no release of the PO fragment could be observed by all phosphorous-containing flame retardants as neat substances. Under the same conditions of measurement the PO-fragment could be detected in flame retardant formulations containing the phosphonate flame retardant PCO 910 in PET. High concentrations of the phosphonate flame retardant lead to a more pronounced maximum of the PO-fragment release. The detection of the PO fragment can be observed at concentrations of PCO 910 in the range of 5 and 10% whereas 2% of PCO 910 results in no detection of the PO fragment. Figure 6 demonstrates the release of PO-fragment for PET containing 10% (left diagram) phosphonate and the correction line of the corresponding phosphate (right diagram) demonstrating no detection of the mass fragment m/z = 47 u which indicates a condensed phase activity of SPDPP in PET. The release of PO-fragments in this experiment setup points out the formation of PO-radicals and a gas phase activity during the combustion process. The generation of PO-radicals allows a recombination reaction of the PO-radicals and high reactive H- or OH-radicals formed during the combustion process intervening the decomposition of the polymer. In this case the detection of m/z = 47 u is very specific for the PO-fragment.
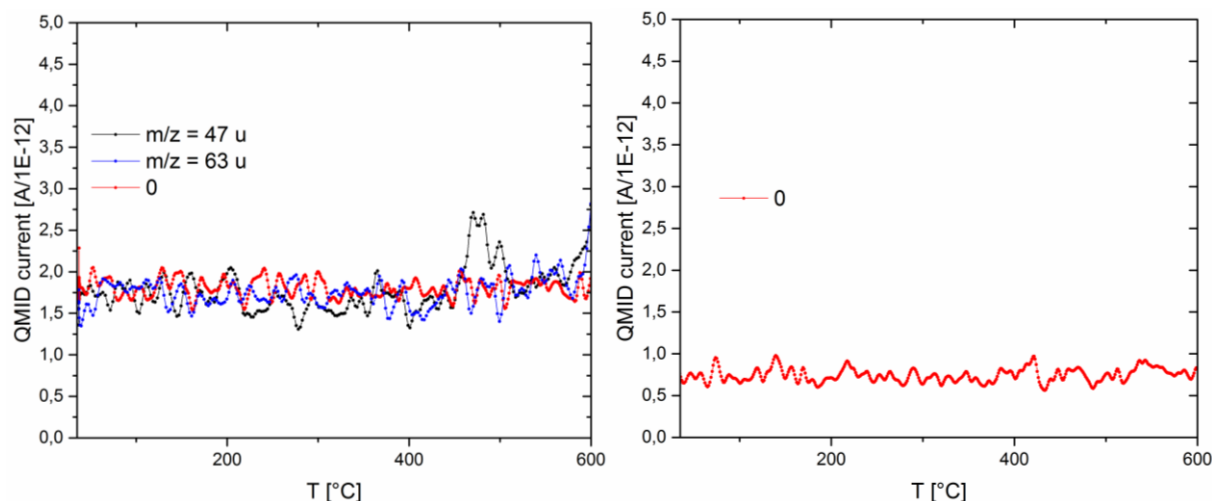
FIGURE 6 FIGURE 7 TG-MS of 10% PCO 910 (left diagram) and 10% SPDPP (right diagram) in PET at 10 K/min under nitrogen. The correction lines of the measurements are marked with 0.

To enhance the gas phase activity of the phosphonate a 1,8-naphthalimide ester (NOR-RF) as NOR radical forming agent was combined with the phosphonate providing different sources of radicals during the combustion process. The expected radical fragment based upon N-O bond-cleavage with m/z = 196 u cannot be detected by TG-MS experiments. The detection of fragments with relatively high molecular weights of more than m/z = 91 u is difficult due to possible condensation in the transfer line. In addition a thermodesorption mass spectrometry experiment was used for pure NOR-RF compound to investigate possible fragmentation reactions. A cleavage mechanism for similar sulfonyl ester of N-hydroxynaphthalimide is already described in the literature.[17] The most important mass fragments are picked in Figure 7 and are in accordance with the mechanism described in the literature by Malval[17b] et al. (Scheme 1). The main fragment of NOR-RF is m/z = 197 u representing a thermodynamically more stable fragment after a hydrogen rearrangement. The main fragments are in accordance to the fragmentation pattern of 1H-benz[de]isoquinoline-1,3(2H)-dione (m/z = 197 u) described in the literature.[18] Due to the experimental setup the onset temperatures of the decomposition in the TD-MS and the TGA-DTA-FTIR-MS experiments are not comparable with each other. The temperatures of the TD-MS experiments are measured in vacuo and thus are representing no exact temperatures of the pyrolysis process.
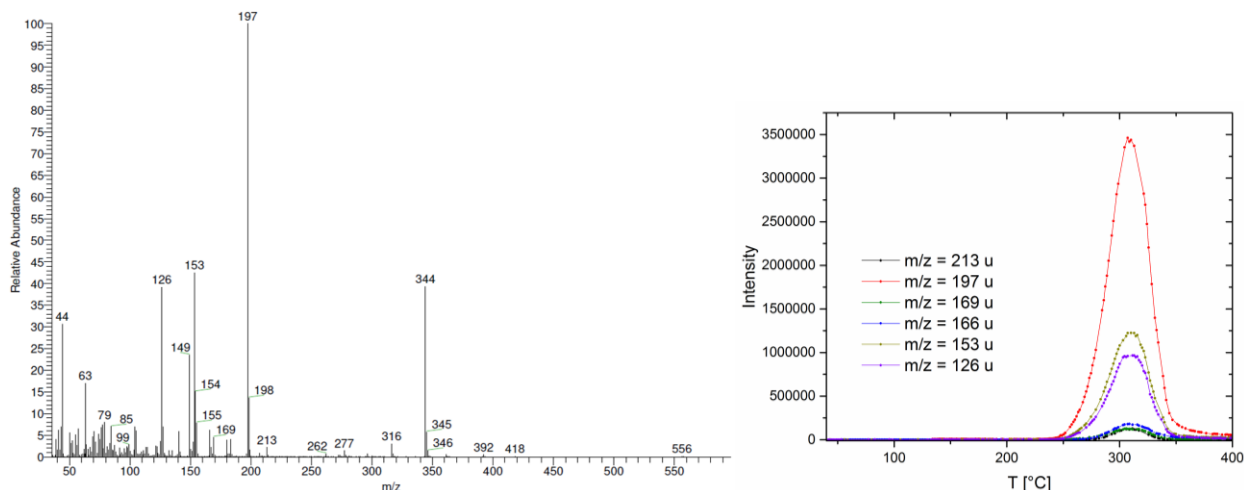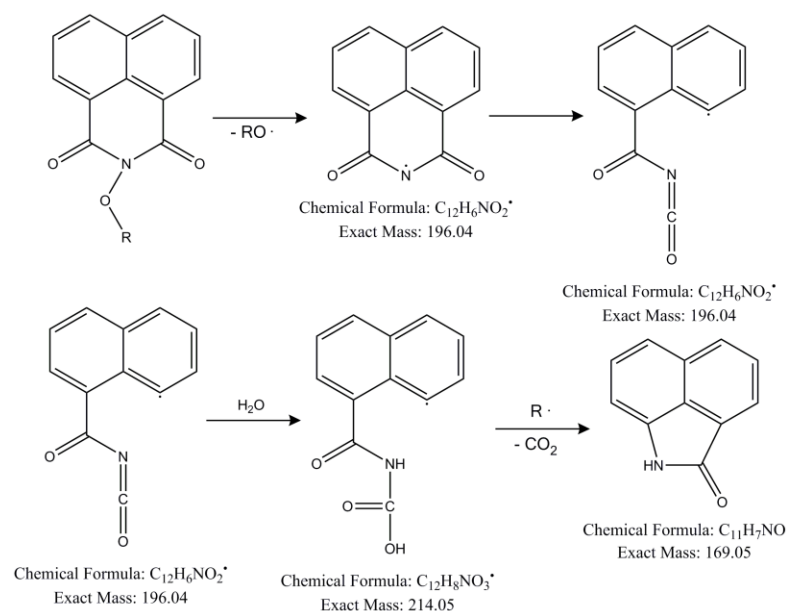
FIGURE 8 Mass spectrum (left) and corresponding thermodesorption mass spectrometry diagram (TD-MS, right). The samples were measured under vacuum with a heating rate of 25 °C/min.

Scheme 1 Radical dissociation mechanism of 1,8-naphthalimide esters described by Malval et al..[17b]

Analysis of the remaining residue at 600 °C

The residues of selected DTA/TGA-MS-FTIR experiments are investigated by SEM-EDX to analyze the approximate phosphorus content in the remaining residues at 600 °C. Spots and areas of the samples were measured with no significant difference. The determination of the P-, C- and O-contents by measurements over areas are listed in Table S1 representing an approximately average content of oxygen, carbon and phosphorus contents of the samples. An exact quantification with SEM-EDX is not possible but the relative phosphorus contents of the samples can be compared to each other. SEM-EDX is a very sensitive method and no unburned samples were measured due to possible contaminations by gas evolution or destruction of the samples by heat development. Neat PCO 910 was not investigated in

this context due to almost no residue remaining at 600 °C. In accordance to previous investigations of this work compositions containing PCO 910 as flame retardant with gas phase activity the phosphorus content of the investigated samples is very low which leads to the conclusion that the main part of the flame retardant is released into the gas phase and thus having an effect in the gas phase. For example, 10% of PCO 910 in PET has a calculated phosphorus content of 2% in the undecomposed sample whereas 0% as phosphorus content remains in the residue at 600 °C. The same amount of the corresponding phenolic phosphate in PET has a phosphorus content of 1% in the residue in comparison to predicted 1% phosphorus content in the undecomposed sample. The main part of the phosphorus content remains in the residue acting in the condensed phase during the decomposition. The combination of the NOR radical forming agent and PCO 910 in PET results in no significant change of the phosphorus or carbon content in the residue at 600 °C. The main part of the phosphorus content of SPDPDOM remains in the condensed phase due to condensed phase active phosphate moieties.

Burning behavior of flame retardant formulations in PET

A UL94 vertical burning test was performed in order to investigate the fire behavior of the developed flame retardant formulations. The results are presented in Table 4. A V-0 classification was reached for samples containing 5% PCO 910, 10% PCO 910 whereas 2% PCO 910 was classified V-2. The fire behavior of 2% PCO 910 as gas phase active flame retardant could be improved by adding 1% NOR-RF. In comparison to that 2% SPDPP as condensed phase active flame retardant in combination with 1% NOR-RF was classified V-2.

TABLE 3 UL94 classification of flame retardant formulations in PET. The thickness of the samples was 1.6 mm.

#	composition	UL94 classification
	PET	n.c.
	2% PCO 910	V-2
	5% PCO 910	V-0
	10% PCO 910	V-0
	2% SPDPP	V-2
	10% SPDPP	V-0
	2% SPDPDOM	V-2
	10% SPDPDOM	V-0
	5% NOR-RF	n.c.
	2% PCO 910 + 1% NOR-RF	V-0
	2% SPDPP + 1% NOR-RF	V-2
	8% PCO 910 + 4% NOR-RF	V-0

CONCLUSIONS

The fire behavior as well as the pyrolysis behavior of different phosphorus species was investigated and compared by insitu thermal analyses of TGA/DTA-FTIR-MS experiments. The PO radical was detected exclusively by compositions containing the phosphonate PCO 910 in PET whereas no PO radical was detected during the decomposition of the neat flame retardants. The corresponding phenolic phosphate in PET showed a condensed phase activity by TGA/DTA-FTIR-MS experiments as well as SEM-EDX experiments investigating the phosphorus content in the remaining residue at 600 °C. The fire behavior of PCO 910 could be improved by adding a NOR radical forming agent (NOR-RF) resulting in a total loading of 3% in PET reaching a V-0 UL94 classification. A new flame retardant SPDPDOM containing phosphate and DOPO moieties was also developed and investigated.

ACKNOWLEDGEMENTS

REFERENCES AND NOTES

[1]   J. Scheirs, in *Modern Polyesters: Chemistry and Technology of Polyesters and Copolyesters*, John Wiley & Sons, Ltd, **2004**, pp. 495-540.
[2]   aX. Xu, J. Sun, Y. Lin, J. Cheng, P. Li, Y. Yan, Q. Shuai, Y. Xie, *Organic & Biomolecular Chemistry* **2017**, *15*, 9875-9879; bM. Aubert, C.-E. Wilén, R. Pfaendner, S. Kniesel, H. Hoppe, M. Roth, *Polymer Degradation and Stability* **2011**, *96*, 328-333.
[3]   aG. Wang, H. Chen, Z. Du, J. Li, Z. Wang, S. Gao, *Science of The Total Environment* **2017**, *590-591*, 50-59; bR. Hou, Y. Xu, Z. Wang, *Chemosphere* **2016**, *153*, 78-90; cI. van der Veen, J. de Boer, *Chemosphere* **2012**, *88*, 1119-1153.
[4]   aA. Lorenzetti, M. Modesti, S. Besco, D. Hrelja, S. Donadi, *Polymer Degradation and Stability* **2011**, *96*, 1455-1461; bU. Braun, A. I. Balabanovich, B. Schartel, U. Knoll, J. Artner, M. Ciesielski, M. Döring, R. Perez, J. K. Sandler, V. Altstädt, *Polymer* **2006**, *47*, 8495-8508.
[5]   aM. M. Velencoso, A. Battig, J. C. Markwart, B. Schartel, F. R. Wurm, *Angewandte Chemie International Edition* **2018**; bD. Y. Wang, *Novel Fire Retardant Polymers and Composite Materials*, Elsevier Science, **2016**; cT. Mariappan, Y. Zhou, J. Hao, C. A. Wilkie, *European Polymer Journal* **2013**, *49*, 3171-3180; dG. J. Minkoff, *Chemistry of combustion reactions*, Butterworths, **1962**; eJ. Green, *Journal of Fire & Flammability* **1996**, *14*, 426-442; fC. A. Wilkie, A. B. Morgan, *Fire Retardancy of Polymeric Materials, Second Edition*, CRC Press, **2009**; gA. I. Balabanovich, D. Pospiech, L. Häußler, C. Harnisch, M. Döring, *Journal of Analytical and Applied Pyrolysis* **2009**, *86*, 99-107.
[6]   M. Sato, S. Endo, Y. Araki, G. Matsuoka, S. Gyobu, H. Takeuchi, *Journal of Applied Polymer Science* **2000**, *78*, 1134-1138.
[7]   O. V. Dolomanov, L. J. Bourhis, R. J. Gildea, J. A. Howard, H. Puschmann, *Journal of Applied Crystallography* **2009**, *42*, 339-341.
[8]   G. M. Sheldrick, *Acta Crystallographica Section A: Foundations of Crystallography* **2008**, *64*, 112-122.
[9]   G. Sheldrick, *Acta Crystallographica Section C* **2015**, *71*, 3-8.
[10]   in *Zeitschrift für Kristallographie - Crystalline Materials, Vol. 209*, **1994**, p. 558.

[11]   aK. Huang, Q. Yao, *Polymer Degradation and Stability* **2015**, *113*, 86-94; bD. Hoang, J. Kim, *Polymer Degradation and Stability* **2008**, *93*, 36-42.

[12]   R. Pfaendner, E. Metzsch-Zilligen, M. STEC, **2014**.

[13]   Z.-S. Zhan, H. Wang, L.-P. Ding, C.-M. Dong, C.-Y. Sun, *3,9-Dichloro-2,4,8,10-tetraoxa-3,9-diphosphaspiro[5.5]undecane-3,9-dione, Vol. 66*, **2010**.

[14]   H. J. Geise, *Recueil des Travaux Chimiques des Pays-Bas* **1967**, *86*, 362-370.

[15]   X.-Z. Guo, L.-S. Wang, *Journal of Chemical & Engineering Data* **2010**, *55*, 4709-4720.

[16]   H. Saeidian, M. Babri, Z. Mirjafary, M. T. Naseri, M. Sarabadani, D. Ashrafi, S. S. M. Faraz, *International Journal of Mass Spectrometry* **2014**, *369*, 59-70.

[17]   aC. J. Martin, G. Rapenne, T. Nakashima, T. Kawai, *Journal of Photochemistry and Photobiology C: Photochemistry Reviews* **2018**, *34*, 41-51; bJ.-P. Malval, F. Morlet-Savary, X. Allonas, J.-P. Fouassier, S. Suzuki, S. Takahara, T. Yamaoka, *Chemical Physics Letters* **2007**, *443*, 323-327.

[18]   N. M. S. D. Center, S. Stein, **2018**.

GRAPHICAL ABSTRACT
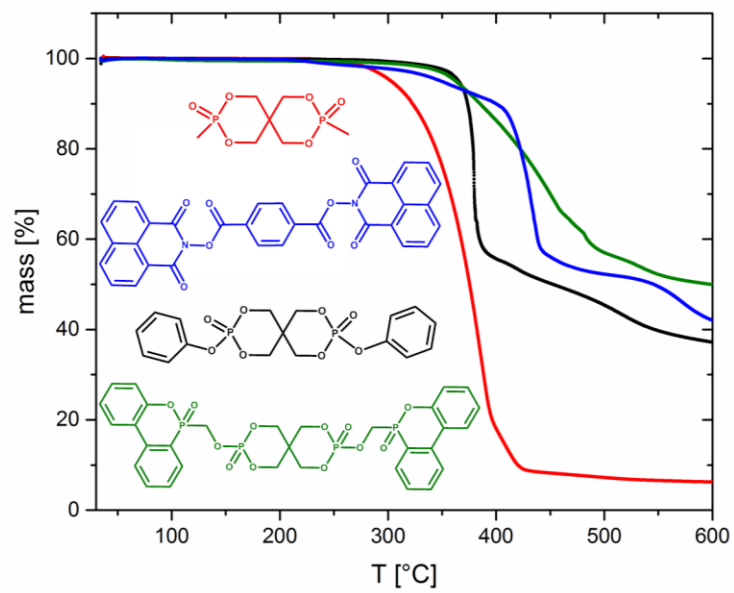
GRAPHICAL ABSTRACT FIGURE ((50 mm wide by 50 mm high, 100 dpi resolution)) .tiff or .eps file format.